

# Defective autophagy associated with LC3 puncta in epothilone-resistant cancer cells

Shensi Shen,<sup>1-3</sup> Oliver Kepp,<sup>1-3</sup> Isabelle Martins,<sup>1-3</sup> Ilio Vitale,<sup>1-3</sup> Sylvie Souquère,<sup>4</sup> Maria Castedo,<sup>1-3</sup> Gérard Pierron<sup>4</sup> and Guido Kroemer<sup>1-3,\*</sup>

<sup>1</sup>INSERM U848; <sup>2</sup>Institut Gustave Roussy; <sup>3</sup>Université Paris Sud-XI; Villejuif, France; <sup>4</sup>CNRS; FRE 2937; Institut Andre Lwoff; Villejuif, France

**Key words:** apoptosis, autophagy, epothilone B, chemotherapy, fibrillar aggregates

**Abbreviations:** DiOC<sub>6</sub>(3), 3,3'-dihexyloxycarbocyanine iodide; GFP, green fluorescent protein; PI, propidium iodine; LC3, microtubule-associated light chain 3; MDR, multidrug resistance

Autophagy is commonly characterized by the redistribution of the microtubule-associated light chain 3 (LC3) protein into cytoplasmic puncta, coinciding with its lipidation, as well as by a decrease in the abundance of autophagic substrates including p62 and ubiquitinated proteins. Here, we describe a cell line, A549-B480, which, in contrast to its parental A549 line, exhibits massive accumulation of LC3 (or a GFP-LC3 fusion protein) in cytoplasmic puncta. These puncta co-localize with accumulated p62 and ubiquitinated proteins, yet are not wrapped by membranes. Indeed, LC3 is not lipidated in A549-B480, even when these cells are cultured in conditions in which A549 cells would develop autophagy. A549-B480 cells have been selected for their resistance against the microtubule-stabilizing agent epothilone B and actually require the continuous presence of epothilone B for their survival. Parental A549 cells treated with epothilone B manifested all signs of bona fide autophagy. In contrast, the autophagic program of A549-B480 was defective, irrespective of the absence or presence of epothilone B, and correlated with the complete absence of Atg7, a protein that is reputed to be essential for autophagy. These results establish novel functional links between microtubules and autophagy, identify a new chemotherapy resistance-associated autophagic defect, and describe the existence of LC3 puncta outside from autophagosomes.

## Introduction

Macroautophagy (hereafter called “autophagy”) is a catabolic process involving the sequestration of portions of the cytoplasm in double-membraned vesicles, autophagosomes, that then fuse with lysosomes to create autolysosomes, in which the luminal content, as well as the internal membrane of the autophagosome are digested.<sup>1,2</sup> Autophagy is most conveniently monitored by measuring the redistribution of the microtubule-associated light chain-3 (LC3) into cytoplasmic dots (which constitute bona fide autophago(lyso)somes), for instance by transfecting cells with a GFP-LC3 fusion protein.<sup>3</sup> Moreover, autophagy can be monitored indirectly by measuring the abundance of p62 (sequestosome 1, SQSTM1)<sup>4</sup> or that of ubiquitinated proteins, which are increased when autophagy is inhibited.<sup>5</sup> Autophagy is generally considered as a cytoprotective mechanism.<sup>1</sup> Multiple anticancer agents including chemotherapeutics and ionizing irradiation induce autophagy that manifests before the tumor cells die. Inhibition of autophagy precipitates the apoptotic or necrotic demise of stressed cells.<sup>6,7</sup> Pharmacological induction of autophagy by non-toxic agents improves cellular resistance to stress and even can prolong the lifespan of whole organisms.<sup>8,9</sup>

Microtubules are dynamic tubulin polymers that can be targeted for the treatment of malignant tumors due to their critical

role in mitosis and other cellular processes.<sup>10</sup> Prominent microtubular inhibitors that are currently used therapeutically are vinca alkaloids (such as vincristine), which destabilize microtubules,<sup>11</sup> and taxanes (such as taxol and paclitaxel), which stabilize microtubules.<sup>11</sup> Although these agents have opposing effects on microtubular dynamics, they induce similar cytotoxic effects on tumor cells in thus far that mitotic arrest is followed by apoptotic cell death.<sup>12</sup> Epothilones constitute a new alternative class of tubulin-binding compounds, which like taxanes stabilize microtubules.<sup>12</sup> In contrast to the currently used taxanes, some epothilones are poorly recognized by P-gp pumps, suggesting that they overcome multidrug resistance (MDR) mechanisms. This has been confirmed in preclinical assays revealing that some paclitaxel- or taxol-resistant cancer can respond to epothilones *in vitro* and *in vivo*.<sup>7</sup> As a result, clinical assays exploring the therapeutic efficacy of epothilones have been initiated.

A549-B480 is a clone of non-small cell lung cancer A549 cells that has been selected by culture in the presence of epothilone B (also called patupilone).<sup>13</sup> Paradoxically, these cells only survive in the continuous presence of 100 to 300 nmol epothilone B because of a series of mutations that lead to amino acid substitutions in class Iβ-tubulin (Gln<sup>292</sup>Glu and Val<sup>60</sup>Phe, in the first and second allele, respectively) and Kα1-tubulin (Leu<sup>195</sup>Met).<sup>13</sup> Upon removal of epothilone B, A549-B480 cells manifest a sequence of alterations

\*Correspondence to: Guido Kroemer; Email: kroemer@orange.fr

Submitted: 10/27/09; Accepted: 10/29/09

Previously published online: [www.landesbioscience.com/journals/cc/article/10468](http://www.landesbioscience.com/journals/cc/article/10468)

(metaphase arrest, abnormal metaphases with monopolar and multipolar spindles, multinucleation, loss of the mitochondrial transmembrane potential, caspase activation, and apoptotic chromatin condensation) that is very similar to those found in normal cells treated with epothilone B.<sup>7</sup> Likewise, this reflects a strong tendency to microtubular destabilization that results from tubulin mutations, yet can be counteracted by epothilone B.

When investigating the effects of taxanes and epothilones on different cancer cell lines, we found that these agents increased the autophagic vacuolization of tumor cells. In contrast to parental A549 cells, A549-B480 manifested the constitutive aggregation of GFP-LC3 in cytoplasmic puncta. This GFP-LC3 aggregation was not affected by the addition or withdrawal of epothilone B. Here, we report that these cells manifest a complete autophagy defect that nevertheless causes the aggregation of GFP-LC3, together with p62 and ubiquitinated proteins, in membrane-free cytoplasmic structures. The autophagy defect of A549-B480 cells correlates with the absence of an essential autophagy-related protein, Atg7. Altogether, these results underscore the likewise functional relationship between microtubule and autophagy in the context of anticancer chemotherapy.

## Results and Discussion

**Accumulation of LC3-GFP protein in membrane-free cytoplasmic aggregates in A549-B480 cells.** Addition of epothilone B to U2OS osteosarcoma cells stably transfected with GFP-LC3 caused the redistribution of GFP-LC3 from a diffuse localization all over the cell (cytoplasm plus nucleus) to an exclusively cytoplasmic, punctate pattern (Fig. 1A and B). A similar GFP-LC3 redistribution was observed in A549 non-small cell lung cancer when they were transiently transfected with GFP-LC3 and then stimulated with epothilone B (not shown). A549 cells treated with epothilone B also manifested the progressive lipidation of LC3, causing an increase in its electrophoretic mobility from the LC3-I to the LC3-II form. This was paralleled by the reduction of p62, in line with the idea that epothilone B triggers bona fide autophagy in A549 cells (Fig. 1C). In strict contrast, A549-B480 cells, which must be cultured in the presence of epothilone B,<sup>13</sup> did not manifest any sign of LC3-I→LC3-II conversion and contained supraphysiological amounts of p62, irrespective of the presence or absence of epothilone B (Fig. 1C), whose withdrawal caused signs of apoptosis such as the dissipation of the mitochondrial transmembrane potential<sup>20,21</sup> followed by plasma membrane permeabilization (Fig. 1D). Transmission electron microscopy revealed electron-dense aggregates in circumscribed cytoplasmic areas from A549-B480 cells. Such structures lacked surrounding membranes or even membrane remnants (Fig. 1E) and were absent in parental A549 cells (not shown). We suspected that these structures might contain GFP-LC3 aggregates. Indeed, immunoelectron microscope revealed immunogold particles that labeled either GFP or p62 within these electron-dense structures, which were often found in the perinuclear area of A549-B480 cells (Fig. 1F). These results indicate that in A549-B480 cells non-lipidated LC3 (or GFP-LC3) accumulates in membrane-free cytoplasmic aggregates.

**Complete autophagy defect in A549-B480 cells due to the absence of Atg7.** To further confirm that LC3 and p62 co-localize in A549-B480 cells, we took advantage of stably GFP-LC3-transfected A549-B480 cells that were fixed, permeabilized and subjected to the immunofluorescence detection of p62. GFP-LC3 and p62 exhibited a strong co-localization in control cells (that were cultured in the continuous presence of epothilone B), in cells in which we attempted to induce autophagy by nutrient depletion (in nutrient-free, NF, medium) or in cells that were deprived from epothilone B. None of these manipulations nor the addition of Bafilomycin A1, a vacuolar ATPase inhibitor that prevents autophagosome/lysosome fusion, did affect the frequency of GFP-LC3 vacuoles, the complete co-localization of GFP-LC3 and p62, or the abundance of p62 protein (Fig. 2A and B). Irrespective of several attempts to induce autophagy (for instance by nutrient starvation in Fig. 2 or by addition of rapamycin, not shown), we found that GFP-LC3 always co-localized with immunoreactive p62 (which is the sum of endogenous LC3 and transfected GFP-LC3), as well as with ubiquitin-positive cytoplasmic structures (Fig. 2C–E). These results could be confirmed by immunoblot experiments performed on A549-B480 cells that lacked GFP-LC3. Irrespective of the continuous presence or withdrawal of epothilone B, A549-B480 cells revealed an abnormally high level of ubiquitinated proteins and the failure to lipidate LC3. These results support the contention that A549-B480 cells are completely autophagy-defective.

To gain insights into the mechanisms of deficient autophagy in A549-B480 cells, we determined the phosphorylation of the mTOR substrate p70<sup>S6K</sup>. Indeed, p70<sup>S6K</sup> was hyperphosphorylated in A549-B480 cells, indicating that the autophagy-inhibitory serine/threonine kinase mTOR is strongly activated. We also measured the phosphorylation of the eukaryotic (translation) initiation factor 2 $\alpha$  (eIF2 $\alpha$ ), which constitutes one of the mandatory checkpoints of autophagy.<sup>22</sup> Surprisingly, phospho-eIF2 $\alpha$  was enhanced in A549-B480 cells as compared to their parental A549 controls, indicating that signals downstream of eIF2 $\alpha$  must explain the autophagy defect of A549-B480 cells. Indeed, we found that the protein Atg7, which is reputed to be essential for autophagy,<sup>1</sup> was completely absent from A549-B480 cells. These results furnish a tentative molecular explanation for the autophagy defect of A549-B480 cells.

## Materials and Methods

**Cell culture and autophagy induction.** A549 non small cell lung cancer cell lines and A549-B480 mutant cell lines were cultured in Dulbecco's Modified Eagle Medium (DMEM)/F-12 medium containing 10% fetal calf serum (FCS), 100 mg/L sodium pyruvate, 10 mM Hepes buffer, 100 units/ml penicillin G sodium and 100  $\mu$ g/ml streptomycin sulfate at 37°C under 5% CO<sub>2</sub>. U2OS osteosarcoma cell lines were cultured in Dulbecco's Modified Eagle Medium containing the same supplements as described above. All media and supplements for cell culture were purchased from Gibco-Invitrogen (Carlsbad, USA). For serum and amino acid starvation, cells were cultured in serum-free Earle's Balanced Salt Solution (Sigma-Aldrich, St. Louis, USA). 10<sup>5</sup> cells were

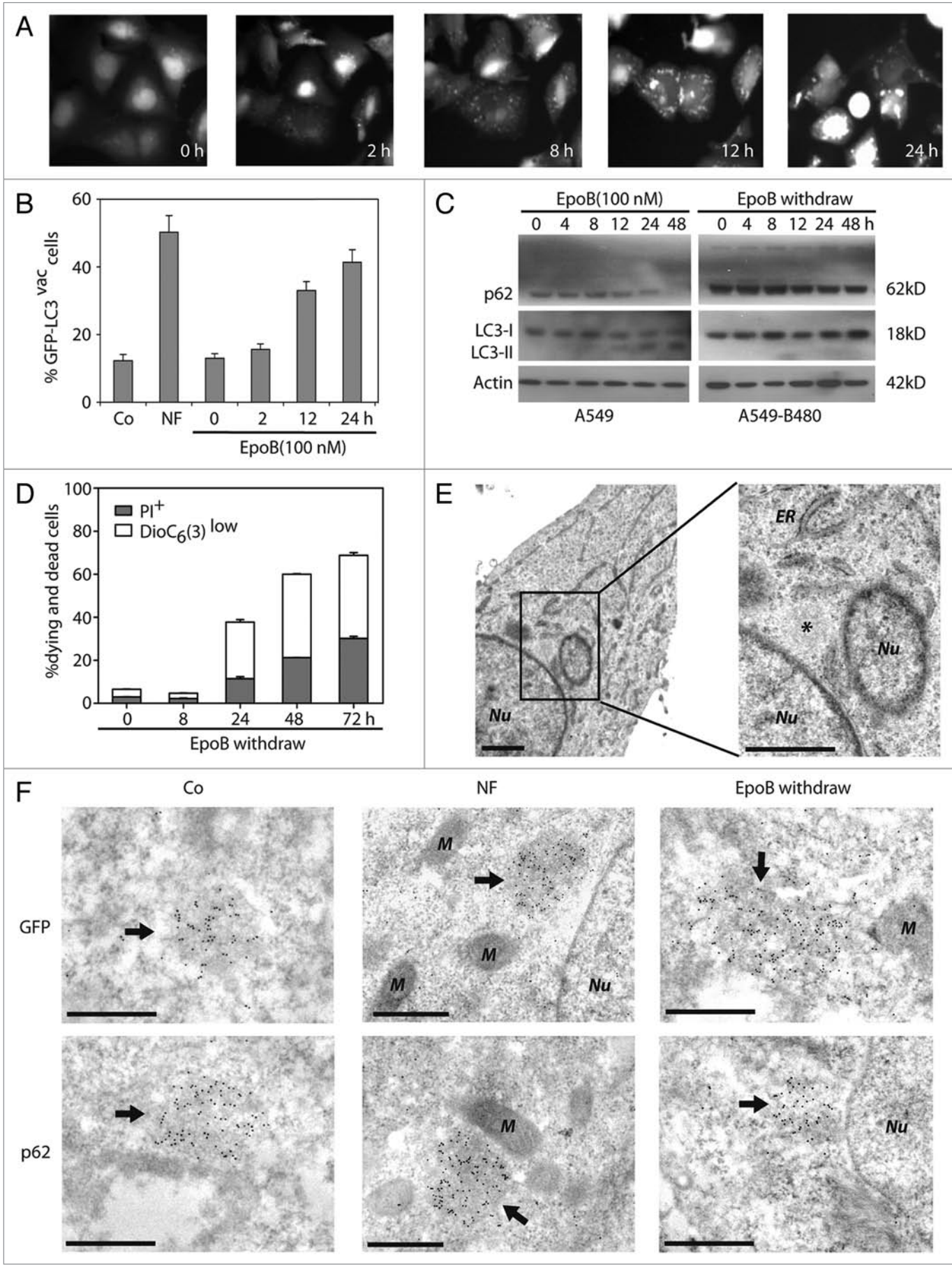


**Figure 1 (See previous page).** Membrane free aggregation of GFP-LC3 in A549-B480 mutant cell lines. (A–C) Epistatic analysis of the effects of Epothilone B (EpoB) on autophagy induction. U2OS cells stably expressing GFP-LC3 were treated with EpoB (100 nM) for the indicated time and the percentage of cells exhibiting GFP-LC3 puncta was determined by fluorescence microscopy (A and B). Alternatively, A549 cells and A549-B480 cells were treated by the addition of Epothilone B (for A549 cells) or withdrawal of Epothilone B (for A549-B480 cells) for the indicated time, and the relative abundance of LC3-I and LC3-II or p62 was determined by immunoblot (C). (D) Cell death in A549-B480 cells is induced upon removal of Epothilone B in a time dependent manner. A549-B480 cells were cultured in Epothilone B free medium for the indicated time and stained with DiOC<sub>6</sub>(3) and PI. The gray and white portions of the columns refer to the DiOC<sub>6</sub>(3)<sup>low</sup>PI<sup>+</sup> (dying) and DiOC<sub>6</sub>(3)<sup>low</sup>PI<sup>-</sup> (dead) population, respectively. (E and F) Ultrastructural evidence of electron-dense finely fibrillar aggregates in A549-B480 cells. A549-B480 cells were cultured in the presence of Epothilone B, fixed in glutaraldehyde and subjected to fixation with embedded in Epon resin. Electron-dense fibrillar, roundish structures were observed by electron microscopy and the representative pictures are shown in (E), bars = 1 μm, Nu: nucleus, ER: endoplasmic reticulum. Star: fibrillar aggregate. Alternatively, cells were embedded in Lowicryl K4M and GFP-LC3 (F upper row) or p62 (F bottom row) were detected, arrows underline highly labeled fibrillar aggregates, M: mitochondria, bars = 0.5 μm.

seeded in 6 well plates and grown for 24 h prior to treatment with epothilone B (EpoB, 100 nM; Tocris), bafilomycin A1 (BafA1, 2 nM, Tocris).

**Immunoblotting.** Cells were lysed on ice in a buffer containing 1% NP40, 20 mM HEPES pH 7.9, 10 mM KCl, 1 mM EDTA, 10% glycerol, 1 mM orthovanadate, 1 mM PMSF, 1 mM dithiothreitol and 10 μg/ml aprotinin, leupeptin and pepstatin before centrifugation (20 min, 14,000 rpm, 4°C) and collection of supernatant. Thereafter, total protein extracts were separated on precast NuPAGE Novex polyacrylamide gels (gradient 10% gels, Invitrogen), and subjected to standard immunoblotting protocols. To this aim, the following specific primary antibodies were employed: anti-p62 (BD Sciences, USA), anti-LC3, anti-ubiquitin, anti-phospho-p70<sup>S6K</sup>, anti-phospho-eIF2 $\alpha$  (all from Cell Signaling), anti-Atg7 (Sigma) or anti-Bec1 (Santa Cruz). The blots were revealed with the appropriate horseradish peroxidase-labeled secondary antibodies (Southern Biotech, Birmingham, USA) and SuperSignal West Pico Chemoluminescent substrate (Pierce Biotechnology, Rockford, USA). Anti-Actin (AbCys, Paris, France) antibody was used to control equal loading.

**Cytofluorometric analysis and immunofluorescence.** Cells were stained with the following probes to assess apoptosis-associated modifications: propidium iodide (1 μg/ml, Sigma-Aldrich) for viability and dihexyloxycarbocyanine iodide [DiOC<sub>6</sub>(3), 40 nmol/L, Molecular Probes-Invitrogen] for  $\Delta\Psi_m$  dissipation.<sup>14–16</sup> After 30 min incubation at 37°C, cells were analyzed using a FACScan equipped with Cell Quest software (Becton Dickinson). For immunofluorescence studies, cells were fixed with paraformaldehyde (4% w/v in PBS) followed by permeabilization using 1% Triton X-100 (Sigma) diluted in phosphate buffered saline (PBS). Cells were stained with specific antibodies against p62 (BD Science, USA), ubiquitin (Cell Signaling) or LC3 (anti-LC3 clone 5F10, nanoTools Antikoerperetechnik, Teningen, Germany) and the nuclei were counterstained with 10 μg/ml Hoechst 33342 (Molecular Probes-Invitrogen). Primary antibodies were revealed either with goat anti-rabbit IgG conjugated to Alexafluor 488 (green) or with goat anti-mouse IgG conjugated to Alexafluor 568 (red) from Molecular Probes-Invitrogen. Fluorescence microscopy determinations were performed by means of a Leica IRE2 microscope equipped with a Leica DC300F camera.

**Quantification of GFP-LC3 puncta.** Autophagy was quantified by counting the percentage of cells showing accumulation of GFP-LC3 in dots (GFP-LC3 puncta, of a minimum of 100

cells per preparation in three independent experiments). Cells presenting a mostly diffuse distribution of GFP-LC3 in the cytoplasm and nucleus were considered non-autophagic, whereas cells representing several intense punctuate GFP-LC3 aggregates were classified as autophagic.<sup>3,17–19</sup>

**Immunoelectron microscopy.** For immunolocalization of GFP-LC3 and p62, glutaraldehyde-fixed Lowicryl-embedded thin sections were first reacted with the primary antibody diluted in PBS for 1 hour at room temperature. After washing in PBS, grids were incubated for 30 min at room temperature with the secondary antibody coupled to 10 nm gold particles, diluted in PBS (goat anti-rabbit for GFP detection; goat anti-mouse for p62 detection). Following final washing in PBS, grids were rapidly rinsed in a jet of distilled water, air-dried, and counterstained with 4% uranyl acetate. Rabbit polyclonal anti-GFP (Abcam 260) and mouse anti-p62 antibodies (BD Science, USA) were used at a dilution of 1/200 and 1/25 respectively and secondary antibodies coupled to 10 nm gold particles (BBInternational) at a dilution of 1/25.

## Concluding Remarks

The results that we include in this report have three major implications.

First, our data hint to novel functional links between microtubules and autophagy. On theoretical grounds, microtubules may impact on autophagy, at several levels. LC3 has been described as a microtubule-associated protein. Since LC3 is a major player in the formation of phagophores (the membrane that progressively enwraps autophagocytic cargo),<sup>23</sup> and LC3 can interact with microtubules,<sup>24</sup> it is tempting to postulate that LC3 must be released from microtubules to participate in the initiation of autophagy. In addition, microtubules may participate in the juxtaposition and later fusion of autophagosomes and lysosomes,<sup>25</sup> meaning that they can influence the late stage of the autophagic process. At present it is not known whether and to which degree, microtubule (de)stabilizing agents impact on the initiation and termination phases of autophagy. Nonetheless, it appears intriguing that a cell line that has been selected for resistance against a microtubule-specific chemotherapeutic agent and that has accumulated several tubulin-specific mutations has developed a complete autophagic defect. It is tempting to speculate that these tubulin mutations (which shift the equilibrium state of the (de)polymerization of tubulin, the microtubular subunits)

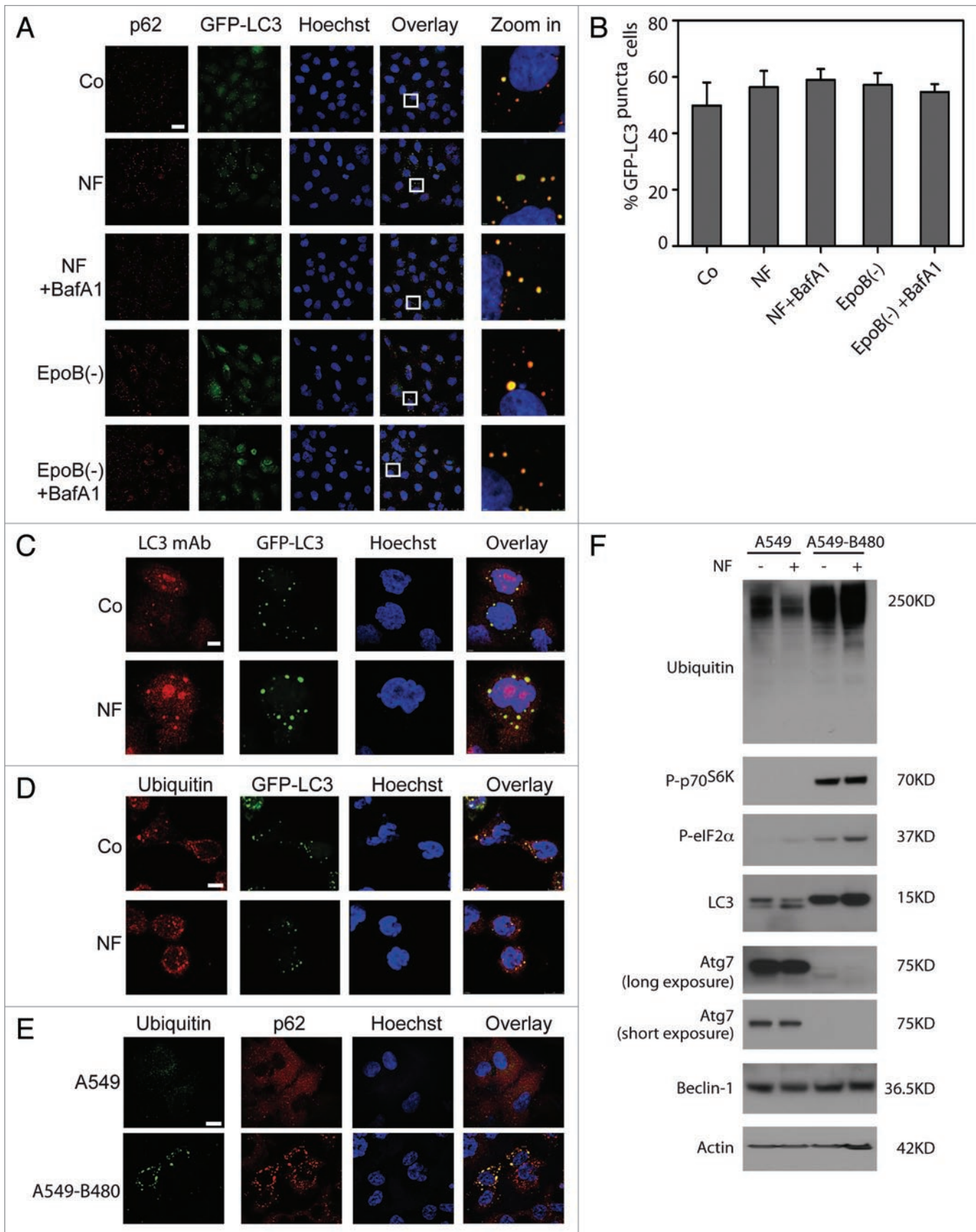


**Figure 2.** For figure legend, see page 6.

**Figure 2.** Autophagy-defect due to the loss of Atg7 expression in A549-B480 mutant cell lines. (A–C) Complete co-localization of LC3 and p62 in the aggregates of A549-B480 cells. Cells were subjected to the indicated treatments for 24 hrs and were stained with anti-p62 antibody, then the frequency of cells with GFP-LC3 puncta was scored (B). Representative pictures are shown in (A), EpoB(-) represents Epothilone B withdrawal. Alternatively, cells were subjected to immunofluorescence analysis for the detection of endogenous LC3 using an monoclonal anti-LC3 antibody (LC3 mAb, 5F10 clone). Representative pictures are shown in (C). (D–F) Absence of Atg7 and dysfunction of autophagy regulation signaling pathways in A549-B480 cells induce accumulation of ubiquitinated proteins. GFP-LC3 stably expressing A549-480 cells were subjected to counterstaining with anti-ubiquitin and Hoechst 33342 for immunofluorescent microscopy (D). A549 cells and A549-B480 cells were subjected to immunofluorescence analysis for the detection of p62 and ubiquitin. Representative immunofluorescence microphotographs are shown in (E). Alternatively, A549-B480 cells were subjected to the indicated treatment. Then the relative abundance of ubiquitin, LC3, Atg7 or Beclin 1 or the phosphorylation levels of p70<sup>S6K</sup> and eIF2 $\alpha$  were determined by immunoblot (F).

are incompatible with a functional autophagic machinery and hence have led to the selection of cells that are defective for macroautophagy.

Second, our results identify a new chemotherapy resistance-associated autophagic defect. A549-B480 cells manifested the hyperactivation of the autophagy-inhibitory mTOR kinase. However, pharmacological inhibition of mTOR with rapamycin failed to induce autophagy in A549-B480 cells (not shown), meaning that the autophagy defect cannot be solely attributed to mTOR activation. Intriguingly, A549-B480 cells completely lacked Atg7 expression at the protein level, while other autophagy-relevant proteins (such as Beclin 1 and Atg5) were normally expressed. The knockout of Atg7 completely abolishes autophagy in several cell types including neurons and hepatocytes *in vivo*,<sup>26</sup> yet has a less pronounced autophagy-suppressive effect on mouse embryonic fibroblasts stimulated with epoxide.<sup>27</sup> However, to our knowledge there has been no report on a “natural” loss of Atg7 suppression, without its genetic manipulation. Whether the loss of Atg7 expression is genetic or epigenetic is elusive. Previously, it has been described that human carcinomas (in particular breast and prostate) are frequently accompanied by loss-of-heterozygosity affecting the *beclin 1* gene,<sup>28</sup> whose product is also essential for autophagy.<sup>1</sup> Indeed, loss of one of the *beclin 1* alleles causes haploinsufficiency and defective autophagy.<sup>28</sup> Whether loss-of-expression occurs in developing or relapsing cancers remains to be investigated.

## References

- Levine B, Kroemer G. Autophagy in the pathogenesis of disease. *Cell* 2008; 132:27-42.
- Yang Z, Klionsky DJ. An overview of the molecular mechanism of autophagy. *Curr Top Microbiol Immunol* 2009; 335:1-32.
- Tasdemir E, Maiuri MC, Orhon I, Kepp O, Morselli E, Criollo A, et al. p53 represses autophagy in a cell cycle-dependent fashion. *Cell Cycle* 2008; 7:3006-11.
- Bjorkoy G, Lamark T, Pankiv S, Overvatn A, Brech A, Johansen T. Monitoring autophagic degradation of p62/SQSTM1. *Methods Enzymol* 2009; 452:181-97.
- Bjorkoy G, Lamark T, Brech A, Outzen H, Perander M, Overvatn A, et al. p62/SQSTM1 forms protein aggregates degraded by autophagy and has a protective effect on huntingtin-induced cell death. *J Cell Biol* 2005; 171:603-14.
- Gonzalez-Polo RA, Boya P, Pauleau AL, Jalil A, Larochette N, Souquere S, et al. The apoptosis/autophagy paradox: autophagic vacuolization before apoptotic death. *J Cell Sci* 2005; 118:3091-102.
- Hoffmann J, Vitale I, Buchmann B, Galluzzi L, Schwede W, Senovilla L, et al. Improved cellular pharmacokinetics and pharmacodynamics underlie the wide anticancer activity of sagopilone. *Cancer Res* 2008; 68:5301-8.
- Yan L, Sadoshima J, Vatner DE, Vatner SE. Autophagy: a novel protective mechanism in chronic ischemia. *Cell Cycle* 2006; 5:1175-7.
- Eisenberg T, Knauer H, Schauer A, Buttner S, Ruckstuhl C, Carmona-Gutierrez D, et al. Induction of autophagy by spermidine promotes longevity. *Nat Cell Biol* 2009.
- Zhou J, Giannakakou P. Targeting microtubules for cancer chemotherapy. *Curr Med Chem Anticancer Agents* 2005; 5:65-71.
- Jordan MA, Kamath K. How do microtubule-targeted drugs work? An overview. *Curr Cancer Drug Targets* 2007; 7:730-42.
- Bekier ME, Fischbach R, Lee J, Taylor WR. Length of mitotic arrest induced by microtubule-stabilizing drugs determines cell death after mitotic exit. *Mol Cancer Ther* 2009; 8:1646-54.
- Yang CP, Verdier-Pinard P, Wang F, Lippaine-Horvath E, He L, Li D, et al. A highly epothilone B-resistant A549 cell line with mutations in tubulin that confer drug dependence. *Mol Cancer Ther* 2005; 4:987-95.
- Hirsch T, Marzo I, Kroemer G. Role of the mitochondrial permeability transition pore in apoptosis. *Biosci Rep* 1997; 17:67-76.
- Marchetti P, Zamzami N, Joseph B, Schraen-Maschke S, Merea-Richard C, Costantini P, et al. The novel retinoid 6-[3-(1-adamantyl)-4-hydroxyphenyl]-2-naphthalene carboxylic acid can trigger apoptosis through a mitochondrial pathway independent of the nucleus. *Cancer Res* 1999; 59:6257-66.
- Ravagnan L, Marzo I, Costantini P, Susin SA, Zamzami N, Petit PX, et al. Lonidamine triggers apoptosis via a direct, Bcl-2-inhibited effect on the mitochondrial permeability transition pore. *Oncogene* 1999; 18:2537-46.
- Tasdemir E, Maiuri MC, Tajeddine N, Vitale I, Criollo A, Vicencio JM, et al. Cell cycle-dependent induction of autophagy, mitophagy and reticulophagy. *Cell Cycle* 2007; 6:2263-7.
- Tasdemir E, Maiuri MC, Galluzzi L, Vitale I, Djavaheri-Mergny M, D'Amelio M, et al. Regulation of autophagy by cytoplasmic p53. *Nat Cell Biol* 2008; 10:676-87.
- Morselli E, Tasdemir E, Maiuri MC, Galluzzi L, Kepp O, Criollo A, et al. Mutant p53 protein localized in the cytoplasm inhibits autophagy. *Cell Cycle* 2008; 7:3056-61.
- Castedo M, Macho A, Zamzami N, Hirsch T, Marchetti P, Uriel J, et al. Mitochondrial perturbations define lymphocytes undergoing apoptotic depletion *in vivo*. *Eur J Immunol* 1995; 25:3277-84.

Third, our results reveal the possible existence of LC3 puncta outside from autophagosomes. Monitoring the redistribution of GFP-LC3 protein to cytoplasmic puncta is a widely employed technique to detect autophagy by video fluorescence microscopy.<sup>29</sup> Similarly, the immunohistochemical detection of endogenous LC3 can be used to assess autophagy in cultured cells or in tissue sections.<sup>30</sup> Our results reveal that the presence of LC3 or GFP-LC3 in cytoplasmic puncta does not necessarily reveal their participation in the formation of phagophores or their accumulation on the membranes from autophagosomes. Thus, our data underscore the importance of performing multiple parallel assays for the detection of autophagy-associated biochemical and ultrastructural changes.<sup>31</sup> Hadn't we performed such complementary assays, we would have concluded that A549-B480 cells exhibit a constitutively active autophagic machinery.

## Acknowledgements

We thank Susan Horvitz, for the gift of epothilone-resistant A549 cells. G.K. is supported by the Ligue Nationale contre le Cancer (Equipes labellisée), Agence Nationale pour la Recherche (ANR), European Commission (Apo-Sys, ChemoRes, ApopTrain), Fondation pour la Recherche Médicale (FRM), Institut National du Cancer (INCa) and Cancéropôle Ile-de-France. S.S. is supported by Apo-Sys, O.K. receives a post-doctoral fellowship from EMBO, I.M. is supported by La Ligue contre le Cancer.

21. Macho A, Castedo M, Marchetti P, Aguilar JJ, Decaudin D, Zamzami N, et al. Mitochondrial dysfunctions in circulating T lymphocytes from human immunodeficiency virus-1 carriers. *Blood* 1995; 86:2481-7.
22. Kouroku Y, Fujita E, Tanida I, Ueno T, Isoai A, Kumagai H, et al. ER stress (PERK/eIF2alpha phosphorylation) mediates the polyglutamine-induced LC3 conversion, an essential step for autophagy formation. *Cell Death Differ* 2007; 14:230-9.
23. Kabeya Y, Mizushima N, Ueno T, Yamamoto A, Kirisako T, Noda T, et al. LC3, a mammalian homologue of yeast Apg8p, is localized in autophagosome membranes after processing. *EMBO J* 2000; 19:5720-8.
24. Halpain S, Dehmelt L. The MAP1 family of microtubule-associated proteins. *Genome Biol* 2006; 7:224.
25. Webb JL, Ravikumar B, Rubinsztein DC. Microtubule disruption inhibits autophagosome-lysosome fusion: implications for studying the roles of aggregates in polyglutamine diseases. *Int J Biochem Cell Biol* 2004; 36:2541-50.
26. Komatsu M, Waguri S, Ueno T, Iwata J, Murata S, Tanida I, et al. Impairment of starvation-induced and constitutive autophagy in Atg7-deficient mice. *J Cell Biol* 2005; 169:425-34.
27. Nishida Y, Arakawa S, Fujitani K, Yamaguchi H, Mizuta T, Kanaseki T, et al. Discovery of Atg5/Atg7-independent alternative macroautophagy. *Nature* 2009; 461:654-8.
28. Qu X, Yu J, Bhagat G, Furuya N, Hibshoosh H, Troxel A, et al. Promotion of tumorigenesis by heterozygous disruption of the beclin 1 autophagy gene. *J Clin Invest* 2003; 112:1809-20.
29. Tasdemir E, Galluzzi L, Maiuri MC, Criollo A, Vitale I, Hangen E, et al. Methods for assessing autophagy and autophagic cell death. *Methods Mol Biol* 2008; 445:29-76.
30. Martinet W, De Meyer GR, Andries L, Herman AG, Kockx MM. Detection of autophagy in tissue by standard immunohistochemistry: possibilities and limitations. *Autophagy* 2006; 2:55-7.
31. Klionsky DJ, Abeliovich H, Agostinis P, Agrawal DK, Aliev G, Askew DS, et al. Guidelines for the use and interpretation of assays for monitoring autophagy in higher eukaryotes. *Autophagy* 2008; 4:151-75.

©2010 Landes Bioscience.  
Do not distribute.